AMPfret: Synthetic nanosensor for cellular energy states

Hannah Crocker[1], Martin Pelosse[1,2,#], Uwe Schlattner[2,3], Imre Berger[1,4*]

[1] Bristol Synthetic Biology Centre BrisSynBio, Biomedical Sciences, School of Biochemistry, University of Bristol, 1 Tankard's Close, Bristol BSH 1TD, United Kingdom.

[2] University of Grenoble Alpes and INSERM U1055, Laboratory of Fundamental and Applied Bioenergetics (LBFA) and SFR Environmental and Systems Biology (BEeSy), Rue de la Piscine, Domaine Universitaire, 38610, Gières, France.

[3] Institut Universitaire de France (IUF), Paris, France.

[4] Max Planck Bristol Centre for Minimal Biology, School of Chemistry, Cantock's Close, Bristol BS8 1TS, UK.

[#] Present address: CEA - Commissariat à l'énergie atomique et aux énergies alternative, 7 Avenue des Martyrs, 38054 Grenoble, France.

[*] Correspondence to: imre.berger@bristol.ac.uk

Abstract:

Cellular energy is a cornerstone of metabolism and is crucial for human health and disease. Knowledge of the cellular energy states and the underlying regulatory mechanisms is therefore key to understanding cell physiology and to design therapeutic interventions. Cellular energy states are characterised by concentration ratios of adenylates, in particular ATP:ADP and ATP:AMP. We applied synthetic biology approaches to design, engineer and validate a genetically encoded nano-sensor for cellular energy state, AMPfret. It employs the naturally evolved energy sensing of eukaryotic cells provided by the AMP-activated protein kinase (AMPK). Our synthetic nano-sensor relies on fluorescence resonance energy transfer (FRET) to detect changes in ATP:ADP and ATP:AMP ratios both *in vitro* and in cells *in vivo*. Construction and iterative optimisation relied on ACEMBL, a parallelised DNA assembly and construct screening technology we developed, facilitated by a method we termed tandem recombineering (TR). Our approach allowed rapid testing of numerous permutations of the AMPfret sensor to identify the most sensitive construct, which we characterised and validated both in the test tube and in cells.

One Sentence Summary:

Rapid DNA assembly and parallelised construct screening tools enabled engineering of a potent FRET-based cellular energy sensor capable of detecting fluctuations in AMP concentrations and ADP/AMP ratios *in vitro* and in cells *in vivo*.

Introduction

Energy metabolism is key to cell survival and homeostasis. Metabolic and energy perturbations have been associated with a wide range of otherwise unrelated human diseases(1–5). A key sensor and regulator of cellular energy metabolism is adenosine monophosphate-activated protein kinase (AMPK), which is ubiquitously expressed and highly conserved throughout evolution(6–12). AMPK is a heterotrimeric serine/threonine kinase, comprising a catalytic subunit, α, and two regulatory subunits, β and γ. AMPK senses the variation in cellular adenylate levels, specifically the ratios of AMP to ATP, and ADP to ATP(13–15). It is activated in response to increases in the AMP:ATP and ADP:ATP ratios during periods of energetic stress, for instance exercise, caloric restriction or ischemia(10,16–18). When the cellular concentration of AMP or ADP rises, these adenylates out-compete ATP for binding to the γ subunit and causes allosteric activation and a defined conformational change(19–21). The activated kinase then re-establishes a correct cellular energy state through the phosphorylation of downstream targets, causing inhibition of anabolic processes and activation of catabolic processes, thereby restoring the levels of ATP as a major energy source.

AMPK has a central role in many metabolic processes and is implicated in many, otherwise unrelated diseases like cancer(22), neurodegenerative(5,23) and kidney diseases(24), rheumatism(25), and notably cardiovascular(26,27) and metabolic diseases(28,29). The kinase is increasingly recognised as a therapeutic target for many of these pathologies, and specific activators are being developed(30–32). Metabolic outcomes mediated by AMPK activation are particularly significant for diabetes mellitus(28,33). AMPK mediates some of the beneficial effects of metformin, the first-line medication for type 2 diabetes (T2D) (34), which activates the kinase indirectly via inhibition of mitochondrial respiratory Complex I and a rise in the ATP/AMP ratio (35,36). Similarly,

AMPK activation in muscle during and after exercise enhances muscle insulin sensitivity (37). In cancer, AMPK may be involved in both the induction and preventing tumours, depending on its metabolic state(22,38). Monitoring AMPK function and modulating cellular energetics by modifying AMPK regulation is thus considered as a key pharmaceutical concept for future therapeutic intervention.

Currently, the predominating experimental methods commonly used to explore the activation state of AMPK are assays using cell and tissue extracts. This mostly includes immunoblotting with phospho-specific antibodies for AMPK or AMPK substrates, but also non-radioactive assays reporting phospho-incorporation into (artificial) substrates(39,40). These methods, however, only provide end-point data that average entire cell populations and that, as in the case of immunoblots, are only semi-quantitative. Immunofluorescence is also used, providing valuable insight into the localisation of the phosphoproteins in single cells. However, this method requires fixation for analysis, again preventing the analysis of living cells, and is not quantitative. Ideally, one would like to follow in time the AMPK activation at the single cell level in response to given stimuli, thus also assaying heterogeneity.

An alternative method is the use of genetically encoded biosensors capable of measuring adenylate levels and ratios in single live cells, ideally by optical methods such as fluorescence resonance energy transfer (FRET). There are an increasing number of genetically encoded FRET biosensors emerging for a range of applications(41–46) including sensors that indirectly gauge AMPK function(47,48). For instance, AMPK Activity Reporter (AMPKAR) consists of a specifically designed, artificial peptide substrate of AMPK and a phosphothreonine-binding forkhead-associated domain 1 (FHA1), attached to a pair of fluorescent proteins capable of FRET(49). Upon AMPK activation, the artificial substrate is phosphorylated and binds to the FHA1 module, juxtaposing the donor and acceptor fluorophores resulting in a detectable FRET signal. AMPKAR and related sensors can also be

successfully targeted to different subcellular compartments(50) or entire animals(51). Nonetheless, these sensors are limited as they neither provide direct, immediate readout on AMPK activity, nor of adenylate ratios, which however are *bona fide* indicators of cellular energy states. Particularly, the available AMPK sensors report the full activation state of AMPK but do not distinguish between the energy-sensing modulation of AMPK phosphorylation by AMP and ADP and covalent activation via phosphorylation/dephosphorylation at the activation loop Thr172(7). They are neither truly reversible, since dephosphorylation of the artificial substrate must be catalysed by cellular phosphatases. A more detailed review of these AMPK substrate FRET sensors can be found in our recent review(47).

To overcome the limitations of existing sensors, we therefore pursued a different approach. We sought to exploit the conformational change upon AMPK activation(19–21) to create a genetically encoded sensor based on AMPK itself, that could faithfully detect and monitor cellular energy states including the ratios between ATP:ADP and ATP:AMP. We reasoned that by attaching fluorophore pairs to the N- and C-termini of the AMPK subunits and testing all possible combinations, we could create a sensitive sensor that would produce a detectable FRET signal without perturbing cell metabolism. To create our AMPK-derived FRET sensor, AMPfret(52), we applied DNA assembly and construct screening methods that we had developed(52–55) facilitating our approach, and we applied protein engineering to optimise our sensor(52). The generation of the AMPfret sensor, and its validation *in vitro* and in cells *in vivo*, are described in the following.

Main Text

Constructing the AMPfret sensor

Our AMPfret sensor is based on the native heterotrimeric AMPK itself, thus directly reporting on AMPK activation mechanisms as naturally evolved in eukaryotes(52). We utilised the $\alpha_2\beta_2\gamma_1$ isoform(56,57), outfitted with two fluorescent proteins at selected protein subunit termini to enable FRET. Upon increase in the cellular AMP:ATP ratio, AMPK undergoes allosteric activation, resulting in a pronounced conformational switch(19,20). In AMPfret, this causes the fluorescent proteins attached to the subunit termini to move in relation to each other, resulting in an increase in FRET. Thus, the FRET output signal detected is directly correlated to the conformational change that occurs on the functional core of the sensor during activation of AMPK.

We required an appropriate expression system to facilitate the generation of the AMPfret sensor. Production of an array of constructs was required to identify which were the best termini to tag with the fluorescent proteins and each would need to be expressed, purified and characterised, first *in vitro* and ultimately within cellular systems *in vivo*. We had previously developed ACEMBL, a method for producing multiprotein complexes in *E. coli*(53). ACEMBL facilitates the rapid assembly of genes into multigene expression cassettes by combining sequence and ligation independent cloning methods (SLIC) and DNA recombination by a site specific recombinase, Cre, in a process we termed tandem recombineering (TR)(55). In TR, genes encoding for subunits of a multiprotein complex are inserted in custom designed minimalistic DNA modules called Acceptor and Donor plasmids, that contain bacterially active promoters (T7, lac), terminators, antibiotic resistance genes, the Cre recombinase recognition site, LoxP and a multiple insertion site (MIE) for inserting the genes of interest at specific restriction sites in a so-called multiplication module, to facilitate multigene assembly. Acceptors contain a regular origin of replication (BR322) that supports

survival in regular *E. coli* cells, while Donors contain a conditional origin of replication derived from the R6Kγ phage(58). Due to the conditional origin, Donors need to be propagated in special *E. coli* cells that express the *pir* gene – for survival in regular *E. coli* cells. In contrast, Donors need to be fused with an Acceptor by Cre-LoxP mediated plasmid fusion for survival in regular strains(54). We cloned each of the three subunits of AMPK in an Acceptor or Donor plasmid, respectively, and tagged each of the six termini (N-terminus, C-terminus) with a fluorescent protein pair capable of FRET, to identify the combination that yielded the highest signal depending on adenylate concentrations (Fig. 1).

We first chose enhanced cyan fluorescent protein (eCFP) and yellow fluorescent protein (YFP) for our experiments as eCFP and YFP constitute a potent FRET pair. In order to identify the most appropriate positions for robust FRET upon activation, all possible permutations were generated (Fig. 1). This involved inserting each AMPK subunit into a separate plasmid, with or without the addition of the fluorescent proteins at either the N- or C-terminus (Fig. 1). Expression and purification of the resulting sensor variants allowed us to identify the most sensitive biosensor, that maximally exploited the conformational changes that are associated with the allosteric activation of AMPK *in vitro* (Fig. 1B,C). More precisely, the α_2 subunit, with or without the donor fluorescent protein, eCFP, at the N- or C-terminus was cloned into the acceptor plasmid, pACE1. To facilitate purification, a DNA encoding for a decahistidine tag and a tobacco etch virus (TEV) protease cleavage site was also inserted at the N-terminus of the construct. The β_2 subunit, likewise with or without the acceptor fluorescent protein, YFP, at the N- or C-terminus was cloned into a donor plasmid, pDC. Finally, the γ_1 subunit was inserted into the donor plasmid pDS (Fig. 1). This final γ_1 subunit was either untagged, or again combined with all possible combinations of the fluorescent proteins at either the N- or C- terminus. The resulting constructs were then fused by their respective LoxP sequences by Cre recombinase (Fig. 1B) to form all possible

variations (AMPfret constructs A to L) of the putative AMPfret sensor (Fig 1D). Restriction mapping of the plasmids, predicted by a software we developed, Cre-ACEMBLER(54), helped to confirm the identity of the fusion plasmids, which were then further confirmed by sequencing. The sensors were then expressed in *E. coli* and purified to homogeneity using immobilised metal affinity (IMAC) using the decahistidine tag, ion exchange chromatography (IEX) and size exclusion chromatography (SEC)(52). All constructs were tested for variation in FRET upon activation with AMP *in vitro*, and a construct comprising an α subunit tagged with eCFP at the C-terminus, a β subunit tagged with YFP at the C-terminus, and a γ subunit that remained untagged was revealed as the best candidate(52). Of note, these sensors were quite insensitive to pH changes and did not respond to guanylates (GMP), as it is the case for AMPK(52).

Optimising AMPfret

We next sought to improve the dynamic range of our sensor by increasing the signal window of the FRET signal produced (Fig. 1C). A range of fluorescent protein pairs capable of FRET exists, each with its own merits, and they are constantly being improved for various characteristics, including quantum yield(46,59). Thus, the eCFP and YFP pair was replaced by the more efficient FRET pair: mseCFP and mVenus.cp173, in order to obtain a sensor more resistant to salt and pH changes(52,60,61). We had designed our original AMPfret constructs such that we could now carry out exchange of fluorophores by traditional restriction digestion and ligation methods by exploiting restriction sites that flanked the fluorescent proteins. Next, we contemplated the flexibility of the fluorophores within the sensor's structure. Secondary structure predictions (nps@consensus, ClustalW2 and psipred servers) conveyed the presence of unstructured amino acid residues at the termini of the AMPK subunits. FRET is highly susceptible to the geometry of the fluorophores with respect to each other. We therefore reasoned that restricting the flexibility of the fluorescent proteins

by removing these disordered residues located at the AMPK subunit termini may be beneficial by reducing the random plasticity in the sensor. We inspected a crystal structure of AMPK (PDBID 2Y94) to define ordered boundaries of the AMPK subunits. Based on this analysis and the secondary structure prediction outputs, we removed two residues (AR) from the C-terminus of the α subunit, three residues (KPI) from the C-terminus of the β subunit and eight residues (LTGGEKKP) from the C-terminus of the γ subunit. This resulted in the α and γ subunits terminating in precisely folded α-helical structures, and the β subunit terminating in a defined β-strand motif. Concomitantly, we also removed the restriction sites we had introduced in our original AMPfret constructs that were used for screening, eliminating two further amino acid residues. These modifications were carried out by PCR-based SLIC procedures(55).

Finally, a further modification was carried out through the addition of a linker sequence forming a particularly rigid α helix, comprising tandem repeats of negatively and positively charged ER/K amino acids(62). We inserted this rigid α helix in between the α subunit and the respective fluorophore attached to it. A corresponding eight amino acid α-helical linker was introduced to quasi 'lock' the fluorophore in place with respect to the AMPK subunits. Thereby, maximally translating the conformational change upon AMPK activation into a FRET signal by restricting the freedom of movement of the donor fluorescent protein with respect to the AMPK complex core and the acceptor fluorophore (Fig. 2A).

The combination of these measures proved to be beneficial and resulted in a significantly improved second-generation AMPfret sensor. The FRET signal difference upon activation substantially increased from approximately 7% to 20%, providing an efficient and reliable genetically encoded biosensor of AMPK activity *in vitro* (Fig. 2B,C)(52).

Deploying the AMPfret sensor *in vivo* in cellular systems

Our ultimate goal was to create a sensitive biosensor that could be applied within cellular systems to provide a faithful optical readout for cellular energetics. Therefore, we investigated the potential of our optimised AMPfret sensor in cells. For this, new constructs were required utilising mammalian active promoters. Our ACEMBL system comprises not only prokaryotic expression reagents, but also plasmids in an identical format that can be used for eukaryotic expression in either insect or mammalian cells. We grafted the genes encoding for our optimised second generation AMPfret biosensor into the mammalian active equivalent plasmids of the ACEMBL suite, MultiMam(63), and applied TR to generate the multigene AMPfret construct for expression of our sensor within mammalian cells. A range of mammalian cell lines including HEK293T, HeLa and 3T3-L1 were transfected and the *in cellulo* activation of AMP was investigated by the addition of known activators of AMPK, AICAR and 2-DG, compellingly validating our approach and the utility of our sensor in cells *in vivo* (Fig. 2D,E). Our experiments yielded important new insight into adenylate-dependent AMPK activation mechanisms(52).

Summary and outlook

By utilising DNA assembly and construct screening technologies we had developed, we created, to the best of our knowledge, the first *bona fide* sensor of cellular energy states. In our experiments, AMPfret proved capable of sensing AMP levels and adenylate ratios, resulting in changes in the detectable FRET signal from the fluorophores attached to AMPK subunit termini, that we engineered for optimal signal intensity. We provided evidence that AMPfret can be used as a robust and effective sensor, for both *in vitro* and in cells *in vivo* applications. The use of this sensor in cells generates many exciting opportunities for future applications. Being able to assess the activation of AMPK within its native environment may

unlock intricate signalling pathways that this kinase is involved in. Moreover, our results firmly set the stage for identifying modulators of AMPK function including small molecule compounds of potential therapeutic benefit in the future. Finally, AMPfret holds the promise of providing a generic probe at the single cell level to analyse adenylate ratios that govern cellular activity in health and disease.

We see ample further scope for optimising AMPfret. The fact that AMPfret consists of three polypeptide chains, which also recombine with cell-endogenous AMPK subunits, does not lead to a detectable decrease in sensitivity. Thus, a primary goal would be to create new versions of the sensor that could be even more sensitive and robust, as well as tailored for specific applications. For example, there is now a wide variety of well characterised fluorescent proteins covering the entire range of the electromagnetic spectrum, from the ultra-violet excitation blue colours, to the infra-red emitting red colours, many of which can be used together as FRET pairs(41,42,59). Such sensors may avoid disturbing endogenous fluorescence due to NADH or other fluorophores in specific cell types. An enhanced FRET signal was already observed when exchanging the FRET pair in both AMPfret variants, however thus far, only blue-yellow FRET pairs have been explored(52). New and emerging FRET biosensors appear to favour more red-shifted FRET pairs, exploiting the potentially larger Forester radii (R_0s) obtained with longer wavelengths(42,64), which may result in a further enhanced FRET efficiency and therefore, an increase in sensitivity. For cellular applications, a further red-shifted donor fluorophore also has the possible advantage that a larger wavelength is used to excite the fluorophore as compared to CFP and its derivatives, utilising a lower energy. This can be beneficial to reduce autofluorescence and phototoxicity of the cells analysed.

Further strategies may include utilising alternative isoforms of the AMPK subunits that may be more suited to specific cell types and may have varying regulation

mechanisms(65,66). Alternative linker strategies could also be considered, with rigid α-helical linkers in between the β subunit and the acceptor fluorophore. This may stabilise a configuration of the fluorophores with increased FRET efficiency upon activation. Another option could be to vary the length of the linkers utilised, to adjust the distance and pitch between the fluorophores in the sensor. In general, iterative rounds of optimisation by permutating fluorophore placement and orientation may be pursued when new fluorescent proteins are inserted into the sensor, to ensure the maximum possible efficiency is obtained.

AMPfret provides a largely homogeneous readout for the cytosolic space, and a weaker signal for the nucleus. Further subcellular localizations identified as crucial for AMPK glucose sensing via fructose-1,6-biphosphate, namely lysosome and mitochondria(67,68), are not visualized so far. Likely, the pool of AMPK (or AMPfret) associated there is limited. Thus, targeted sensors are needed, which are easily conceivable(50) by supplying organelle and cell compartment specific tags. Similarly, cell type specific promoters can provide AMPfret expression in a specific subset of cells in a tissue.

All these and further modifications are greatly facilitated by the modular nature of the ACEMBL system utilised here for iterative sensor construction (Fig. 1A-C). With the subunits present in separate plasmids, their manipulation is straight forward, as is the regeneration of the complete, sensor encoding construct by Cre recombinase mediated plasmid fusion. We anticipate an entire tool-kit of AMPfret-derived sensors, each with customised properties, ready to probe energy states and uncover functional mechanisms in a multitude of cell functions and disease states.

Perspectives

- Cellular energy states are key indicators of cell function, in health and disease.
- Based on the metabolic hub AMPK, we developed our genetically encoded synthetic sensor, AMPfret, to monitor energy states by faithfully measuring adenylate ratios *in vitro* and in cells *in vivo*.
- Biochemical and biophysical characterisation of AMPfret revealed novel mechanisms of AMPK activation.
- Based on our results, we envisage a tool-kit of tailored AMPfret biosensors with diverse properties, for a multitude of applications, including screening for small molecule compounds for future therapeutic interventions by targeting cell energetics.

Acknowledgment

We thank all members of the Berger and Schlattner teams for their contributions and stimulating discussions. We acknowledge support from the French regional government of Rhône-Alpes *(CIBLE*), the French National Research Agency ANR (*Investissements d'Avenir* ANR-15-IDEX-02), the European Commission (EC) project ComplexINC (Contract Nr. 613879), as well as BrisSynBio, a BBSRC/EPSRC Research Centre for synthetic biology at the University of Bristol (BB/L01386X/1).

Author Contributions

H.C., M.P., U.S. and I.B. prepared the manuscript together.

Competing Interest Statement

M.P., U.S. and I.B. declare competing interest. I.B. is inventor on patents relating to the ACEMBL technology and is co-founder and shareholder of Geneva Biotech SARL, Switzerland, commercialising ACEMBL and its applications. Moreover, M.P., I.B. and U.S. are inventors on a patent application describing AMPfret applications.

References

1. DeBerardinis RJ, Thompson CB. Cellular Metabolism and Disease: What Do Metabolic Outliers Teach Us? Cell. 2012;148(6):1132–44.
2. Le A, Udupa S, Zhang C. The Metabolic Interplay between Cancer and Other Diseases. Trends in Cancer. 2019;5(12):809–21.
3. Wallace DC. A mitochondrial bioenergetic etiology of disease. J Clin Invest. 2013;123(4):1405–12.
4. Neubauer S. The Failing Heart - An Engine Out of Fuel. N Engl J Med. 2007;356:1140–51.
5. Xu J, Begley P, Church SJ, Patassini S, Hollywood KA, Jüllig M, et al. Graded perturbations of metabolism in multiple regions of human brain in Alzheimer's disease: Snapshot of a pervasive metabolic disorder. Biochim Biophys Acta - Mol Basis Dis. 2016;1862(6):1084–92.
6. Hardie DG, Ross FA, Hawley SA. AMPK: a nutrient and energy sensor that maintains energy homeostasis. Nat Rev Mol Cell Biol. 2012;13(4):251–62.
7. Hardie DG. Keeping the home fires burning: AMP-activated protein kinase. J R Soc Interface. 2018;15(138):1–23.
8. Herzig S, Shaw RJ. AMPK: Guardian of metabolism and mitochondrial homeostasis. Vol. 19, Nature Reviews Molecular Cell Biology. 2018. p. 121–35.
9. Lin SC, Hardie DG. AMPK: Sensing Glucose as well as Cellular Energy Status. Vol. 27, Cell Metabolism. 2018. p. 299–313.
10. Carling D. AMPK signalling in health and disease. Curr Opin Cell Biol. 2017;45:31–7.
11. Garcia D, Shaw RJ. AMPK: Mechanisms of Cellular Energy Sensing and Restoration of Metabolic Balance. Mol Cell. 2017;66(6):789–800.

12. Kurumbail RG, Calabrese MF. Structure and Regulation of AMPK. EXS. 2016;107:3–22.
13. Gowans GJ, Hawley SA, Ross FA, Hardie DG. AMP Is a True Physiological Regulator of AMP-Activated Protein Kinase by Both Allosteric Activation and Enhancing Net Phosphorylation. Cell Metab. 2013;18(4):556–66.
14. Xiao B, Sanders MJ, Underwood E, Heath R, Mayer F V., Carmena D, et al. Structure of mammalian AMPK and its regulation by ADP. Nature. 2011;472(7342):230–3.
15. Oakhill JS, Steel R, Chen ZP, Scott JW, Ling N, Tam S, et al. AMPK is a direct adenylate charge-regulated protein kinase. Science. 2011;332(6036):1433–5.
16. Steinberg GR, Kemp BE. AMPK in Health and Disease. Physiol Rev. 2009;89(3):1025–78.
17. Kjøbsted R, Hingst JR, Fentz J, Foretz M, Sanz MN, Pehmøller C, et al. AMPK in Skeletal muscle function and metabolism. FASEB J. 2018;32(4):1741–77.
18. Qi D, Young LH. AMPK: Energy sensor and survival mechanism in the ischemic heart. Trends Endocrinol Metab. 2015;26(8):422–9.
19. Riek U, Scholz R, Konarev P, Rufer A, Suter M, Nazabal A, et al. Structural properties of AMP-activated protein kinase: dimerization, molecular shape, and changes upon ligand binding. J Biol Chem. 2008;283(26):18331–43.
20. Chen L, Wang J, Zhang Y-Y, Yan SF, Neumann D, Schlattner U, et al. AMP-activated protein kinase undergoes nucleotide-dependent conformational changes. Nat Struct Mol Biol. 2012;19(7):716–8.
21. Zhu L, Chen L, Zhou XM, Zhang YY, Zhang YJ, Zhao J, et al. Structural insights into the architecture and allostery of full-length AMP-activated protein kinase. Structure. 2011;19(4):515–22.
22. Vara-Ciruelos D, Russell FM, Grahame Hardie D. The strange case of AMPK and

cancer: Dr Jekyll or Mr Hyde? Open Biol. 2019;9(7):1–21.

23. Curry DW, Stutz B, Andrews ZB, Elsworth JD. Targeting AMPK Signaling as a Neuroprotective Strategy in Parkinson's Disease. J Parkinsons Dis. 2018;8:161–81.
24. Rajani R, Pastor-Soler NM, Hallows KR. Role of AMP-activated protein kinase in kidney tubular transport, metabolism, and disease. Curr Opin Nephrol Hypertens. 2017;26(5):375–83.
25. McHugh J. AMPK: a therapeutic target in RA? Nat Rev Rheumatol. 2019;15(4):188.
26. Li X, Liu J, Lu Q, Ren D, Sun X, Rousselle T, et al. AMPK: a therapeutic target of heart failure - not only metabolism regulation. Biosci Rep. 2019;39(1):1–13.
27. Pelosse M, Tokarska-Schlattner M, Schlattner U. AMP-activated protein kinase: A metabolic stress sensor in the heart. In: Cardiac Cytoarchitecture: How to Maintain a Working Heart. Springer, Cham; 2015. p. 187–225.
28. Day EA, Ford RJ, Steinberg GR. AMPK as a Therapeutic Target for Treating Metabolic Diseases. Trends Endocrinol Metab. 2017;28(8):545–60.
29. Ruderman NB, Carling D, Prentki M, Cacicedo JM. AMPK, insulin resistance, and the metabolic syndrome. J Clin Invest. 2013;123(7):2764–72.
30. Olivier S, Foretz M, Viollet B. Promise and challenges for direct small molecule AMPK activators. Biochem Pharmacol. 2018;153:147–58.
31. Steinberg GR, Carling D. AMP-activated protein kinase: the current landscape for drug development. Nat Rev Drug Discov. 2019;18:527–51.
32. Guigas B, Viollet B. Targeting AMPK: From Ancient Drugs to New Small-Molecule Activators. EXS. 2016;107:327–50.
33. Coughlan KA, Valentine RJ, Ruderman NB, Saha AK. AMPK activation: A therapeutic target for type 2 diabetes? Diabetes, Metab Syndr Obes Targets Ther. 2014;7:241–53.

34. Foretz M, Guigas B, Viollet B. Understanding the glucoregulatory mechanisms of metformin in type 2 diabetes mellitus. Nat Rev Endocrinol. 2019;15(10):569–89.
35. Foretz M, Hébrard S, Leclerc J, Zarrinpashneh E, Soty M, Mithieux G, et al. Metformin inhibits hepatic gluconeogenesis in mice independently of the LKB1/AMPK pathway via a decrease in hepatic energy state. J Clin Invest. 2010;120(7):2355–69.
36. El-Mir MY, Nogueira V, Fontaine E, Avéret N, Rigoulet M, Leverve X. Dimethylbiguanide inhibits cell respiration via an indirect effect targeted on the respiratory chain complex I. J Biol Chem. 2000;275(1):223–8.
37. Viollet B. The energy sensor AMPK: Adaptations to exercise, nutritional and hormonal signals. In: Spiegelman B (eds.) Hormones, metabolism and the benefits of exercise. Research and Perspectives in Endocrine Interactions. Springer, Cham. (2017)
38. Evans JMM, Donnelly LA, Emslie-Smith AM, Alessi DR, Morris AD. Metformin and reduced risk of cancer in diabetic patients. Br Med J. 2005;330:1304–5.
39. Hawley SA, Fyffe FA, Russell FM, Gowans GJ, Grahame Hardie D. Intact cell assays to monitor AMPK and determine the contribution of the AMP-binding or ADaM sites to activation. In: Neumann D, Viollet B, editors. Methods in Molecular Biology. Humana Press Inc.; 2018. p. 239–53.
40. Fyffe FA, Hawley SA, Gray A, Hardie DG. Cell-free assays to measure effects of regulatory ligands on AMPK. In: Neumann D, Viollet B, editors. Methods in Molecular Biology. Humana Press Inc.; 2018. p. 69–86.
41. Lindenburg L, Merkx M. Engineering genetically encoded FRET sensors. Sensors. 2014;14(7):11691–713.
42. Schaaf T, Li A, Grant B, Peterson K, Yuen S, Bawaskar P, et al. Red-Shifted FRET Biosensors for High-Throughput Fluorescence Lifetime Screening. Biosensors. 2018;8(4):1–15.

43. Algar WR, Hildebrandt N, Vogel SS, Medintz IL. FRET as a biomolecular research tool — understanding its potential while avoiding pitfalls. Nat Methods. 2019;16(9):815–29.
44. Maryu G, Miura H, Uda Y, Komatsubara AT, Matsuda M, Aoki K. Live-cell Imaging with Genetically Encoded Protein Kinase Activity Reporters. Cell Struct Funct. 2018;43(1):61–74.
45. Marx V. Probes: FRET sensor design and optimization. Nat Methods. 2017;14(10):949–53.
46. Hochreiter B, Pardo-Garcia A, Schmid J. Fluorescent Proteins as Genetically Encoded FRET Biosensors in Life Sciences. Sensors. 2015;15(10):26281–314.
47. Pelosse M, Cottet-Rousselle C, Grichine A, Berger I, Schlattner U. Genetically Encoded Fluorescent Biosensors to Explore AMPK Signaling and Energy Metabolism. In: Cordero M, Viollet B, editors. AMP-activated Protein Kinase Experientia Supplementum. 2016. p. 491–523.
48. Miyamoto T, Rho E, Kim A, Inoue T. Cellular Application of Genetically Encoded Sensors and Impeders of AMPK. In: Neumann D, Viollet B, editors. AMPK Methods in Molecular Biology. Humana Press, New York, NY; 2018. p. 255–72.
49. Tsou P, Zheng B, Hsu C-H, Sasaki AT, Cantley LC. A Fluorescent Reporter of AMPK activity and Cellular Energy Stress. Cell Metab. 2011;13(4):476–86.
50. Miyamoto T, Rho E, Sample V, Akano H, Magari M, Ueno T, et al. Compartmentalized AMPK Signaling Illuminated by Genetically Encoded Molecular Sensors and Actuators. Cell Rep. 2015;11(4):657–70.
51. Konagaya Y, Terai K, Sumiyama K, Asano T, Correspondence MM. A Highly Sensitive FRET Biosensor for AMPK Exhibits Heterogeneous AMPK Responses among Cells and Organs. Cell Rep. 2017;21:2628–38.
52. Pelosse M, Cottet-Rousselle C, Bidan CM, Dupont A, Gupta K, Berger I, et al. Synthetic

energy sensor AMPfret deciphers adenylate-dependent AMPK activation mechanism. Nat Commun. 2019;10(1):1–13.

53. Bieniossek C, Nie Y, Frey D, Olieric N, Schaffitzel C, Collinson I, et al. Automated unrestricted multigene recombineering for multiprotein complex production. Nat Methods. 2009;6(6):447–52.

54. Nie Y, Chaillet M, Becke C, Haffke M, Pelosse M, Fitzgerald D, et al. ACEMBL Tool-Kits for High-Throughput Multigene Delivery and Expression in Prokaryotic and Eukaryotic Hosts. In: Vega M, editor. Advanced Technologies for Protein Complex Production and Characterization. 896th ed. Springer, Cham; 2016. p. 27–42.

55. Haffke M, Viola C, Nie Y, Berger I. Tandem Recombineering by SLIC Cloning and Cre-LoxP Fusion to Generate Multigene Expression Constructs for Protein Complex Research. Synth Biol. 2013;1073:131–40.

56. Neumann D, Woods A, Carling D, Wallimann T, Schlattner U. Mammalian AMP-activated protein kinase: Functional, heterotrimeric complexes by co-expression of subunits in Escherichia coli. Protein Expr Purif. 2003;30(2):230–7.

57. Suter M, Riek U, Tuerk R, Schlattner U, Wallimann T, Neumann D. Dissecting the role of 5′-AMP for allosteric stimulation, activation, and deactivation of AMP-activated protein kinase. J Biol Chem. 2006;281(43):32207–16.

58. Penfold RJ, Pemberton JM. An improved suicide vector for construction of chromosomal insertion mutations in bacteria. Gene. 1992;118(1):145–6.

59. Bajar BT, Wang ES, Zhang S, Lin MZ, Chu J, Hildebrandt N, et al. A Guide to Fluorescent Protein FRET Pairs. Sensors. 2016;16(1488):1–24.

60. Llopis J, McCaffery JM, Miyawaki A, Farquhar MG, Tsien RY, Kato-Yamada Y, et al. Measurement of cytosolic, mitochondrial, and Golgi pH in single living cells with green fluorescent proteins. Proc Natl Acad Sci U S A. 1998;95(12):6803–8.

61. Imamura H, Nhat KPH, Togawa H, Saito K, Iino R, Kato-Yamada Y, et al. Visualization of ATP levels inside single living cells with fluorescence resonance energy transfer-based genetically encoded indicators. Proc Natl Acad Sci U S A. 2009;106(37):15651–6.
62. Sivaramakrishnan S, Spink BJ, Sim AYL, Doniach S, Spudich JA. Dynamic charge interactions create surprising rigidity in the ER/K alpha-helical protein motif. Proc Natl Acad Sci U S A [Internet]. 2008 [cited 2019 Sep 24];105(36):13356–61. Available from: http://www.ncbi.nlm.nih.gov/pubmed/18768817
63. Kriz A, Schmid K, Baumgartner N, Ziegler U, Berger I, Ballmer-Hofer K, et al. A plasmid-based multigene expression system for mammalian cells. Nat Commun. 2010;1(120):1–6.
64. Bajar BT, Wang ES, Lam AJ, Kim BB, Jacobs CL, Howe ES, et al. Improving brightness and photostability of green and red fluorescent proteins for live cell imaging and FRET reporting. Sci Rep. 2016;6(20889):1–12.
65. Ross FA, Jensen TE, Hardie DG. Differential regulation by AMP and ADP of AMPK complexes containing different γ subunit isoforms. Biochem J. 2016;473:189–99.
66. Willows R, Navaratnam N, Lima A, Read J, Carling D. Effect of different γ-subunit isoforms on the regulation of AMPK. Biochem J. 2017;474:1741–54.
67. Zhang CS, Hawley SA, Zong Y, Li M, Wang Z, Gray A, et al. Fructose-1,6-bisphosphate and aldolase mediate glucose sensing by AMPK. Nature. 2017; 548(7665):112–6.
68. Zong Y, Zhang CS, Li M, Wang W, Wang Z, Hawley SA, et al. Hierarchical activation of compartmentalized pools of AMPK depends on severity of nutrient or energy stress. Cell Res. 2019;29(6):460–73.

Figures and Legends

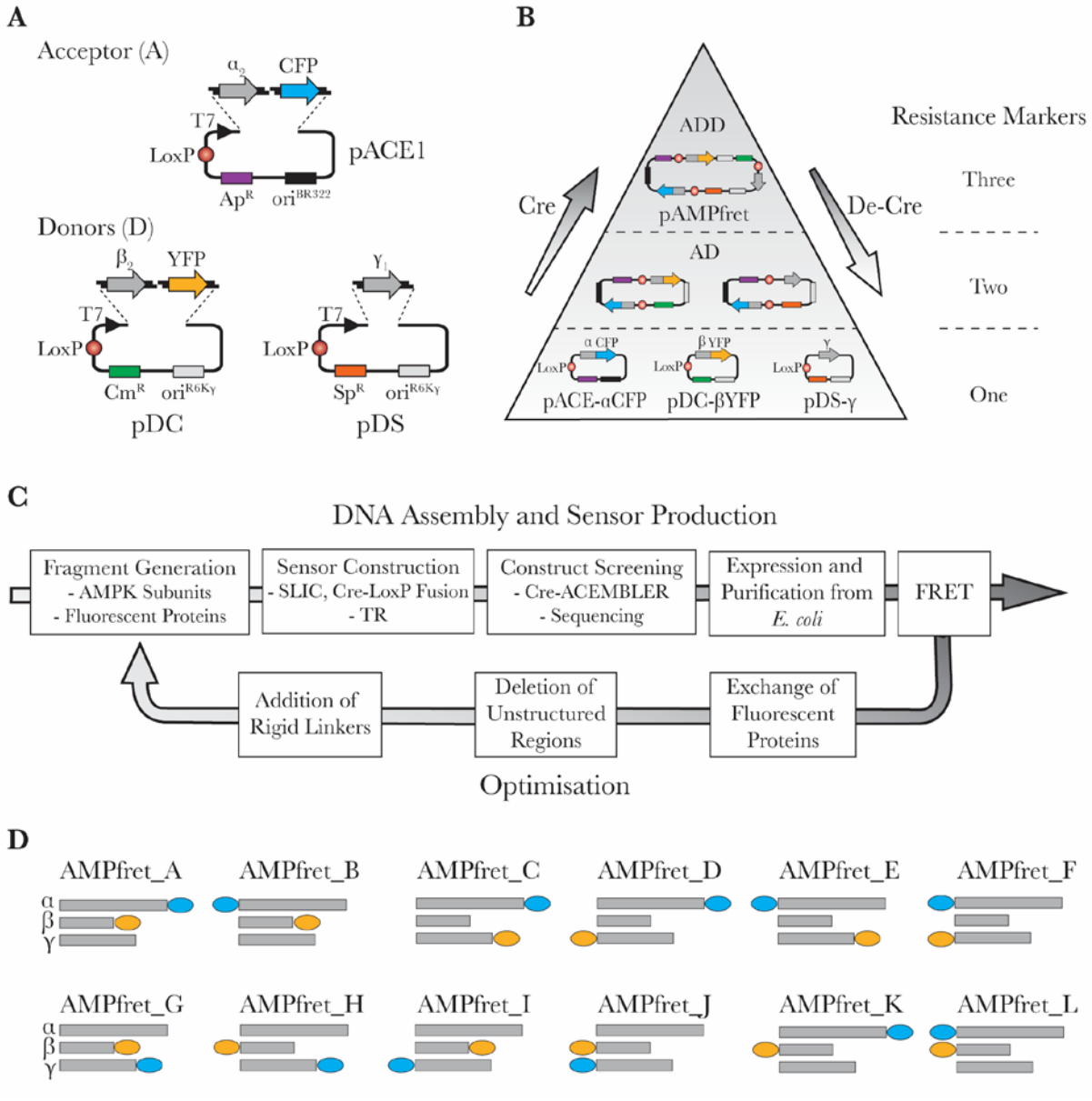

Figure 1. Constructing biosensor AMPfret. (**A**) AMPfret was expressed in *E. coli* and purified. The α subunit of AMPK and a fluorescent protein (YFP) were cloned into pACE1, a so-called Acceptor plasmid module from the ACEMBL suite(52,53). The β subunit of AMPK and a second fluorescent protein (CFP) was cloned into pDC, and the γ subunit of AMPK was cloned into pDS, respectively. pDS and pDC are so-called Donor plasmids in the ACEMBL suite(52,53). The Cre recombinase recognition site, LoxP, is shown as a red circle; the T7 prokaryotic promoter as a black triangle; the genes encoding for antibiotic resistance in

coloured rectangles. Origins of replication, BR322 and R6Kγ, are displayed as black and grey boxes, respectively. CFP, cyan fluorescent protein; YFP, yellow fluorescent protein; Ap, ampicillin; Cm, chloramphenicol; Sp, spectinomycin; ori, origin of replication. (**B**). Multigene expression constructs are prepared from Donor and Acceptor plasmids by Cre-LoxP plasmid fusion mediated by the Cre recombinase. Acceptor-donor fusions (AD) and the acceptor-donor-donor (ADD) fusion are identified by the resistance marker combinations. ADD fusion pAMPfret comprises the genes encoding for the heterotrimeric sensor including the functional FRET pair. (**C**). ACEMBL high throughput pipeline utilised for the generation of AMPfret sensors. The desired genes encoding for the AMPK subunits and fluorescent proteins were inserted into the respective acceptor and donor plasmid backbones by SLIC and combined Cre-LoxP fusion. This process is termed tandem recombineering (TR). Fusion constructs are then screened by fusion plasmid restriction mapping, facilitated by the Cre-ACEMBLER software, and correct clones confirmed by DNA sequencing. AMPfret variants are expressed and purified and followed by *in vitro* characterisation analysing changes in FRET signal upon activation. This process is iteratively repeated and the sensor optimised whereby components such as the fluorescent proteins and linker regions are modified. (**D**). Schematic depicting the topology of AMPfret variants initially constructed for testing. CFP and YFP are represented as blue and yellow ovals respectively. AMPK subunits, α, β and γ are shown as labelled grey rectangles.

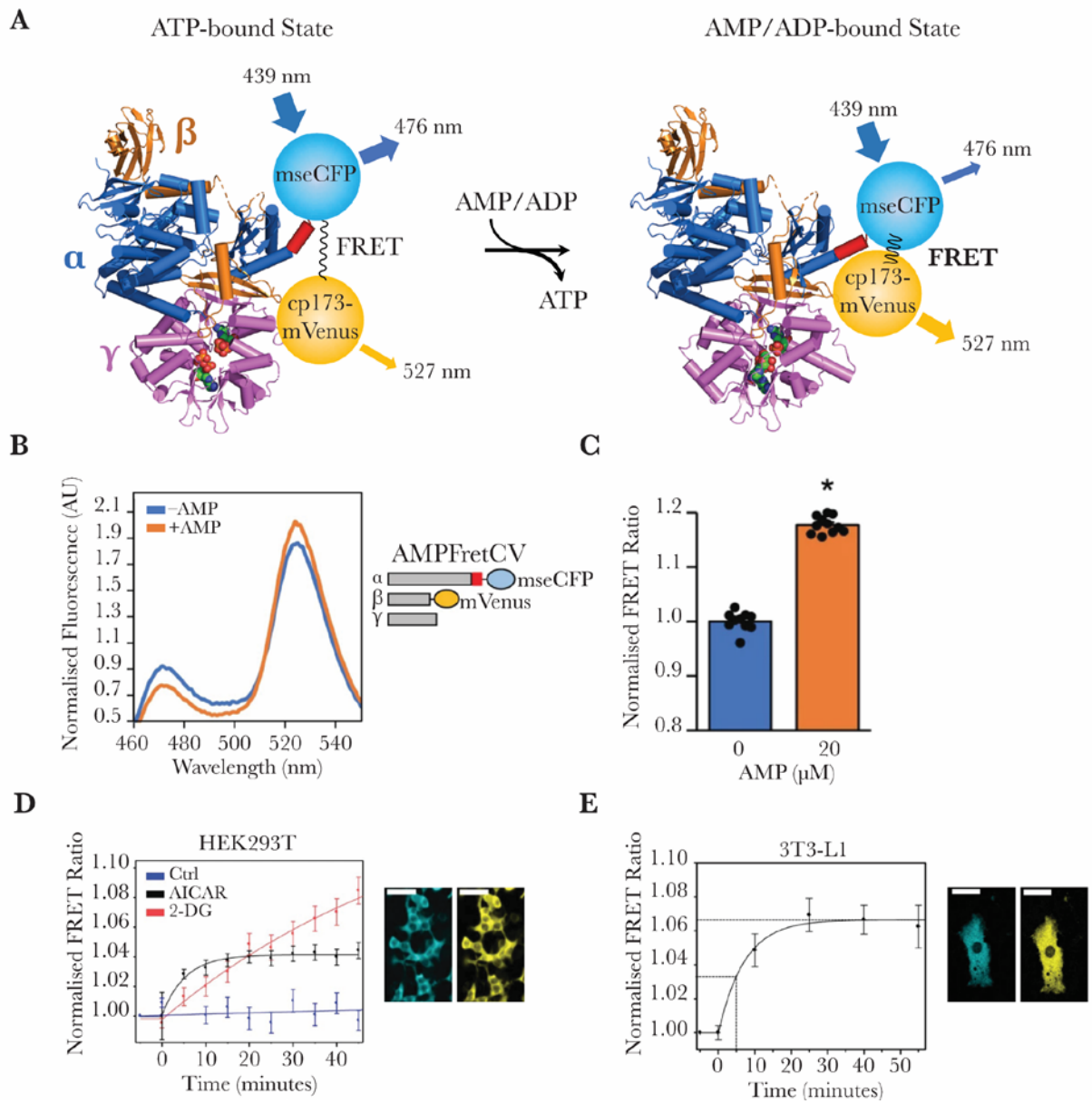

528

529 **Figure 2. Characterisation of AMPfret *in vitro* and in cells *in vivo*.** (**A**) The optimized
530 AMPfret biosensor is shown in a cartoon representation illustrating the mode of action upon
531 sensor activation. The structure shown is based on heterotrimeric AMPK with subunits α, β
532 and γ coloured blue, orange and magenta, respectively. The fluorescent protein mseCFP is
533 shown as a blue circle, a small rigid α-helical linker is coloured in red and the fluorescent
534 protein cp173-mVenus is shown as a yellow circle. A conformational change occurs
535 following the binding of AMP or ADP to the γ subunit, resulting in FRET signal change.
536 Excitation and emission wavelengths are shown for each fluorophore. The model was based

on AMPK crystal structures (PDB ID 4EAK, 4EAI and 5ISO), bound AMP is drawn in a space filling representation. (**B)** *In vitro* characterisation of AMPfret showing a positive change in FRET upon activation with AMP. Bars coloured in grey depict AMPfret subunits. The rigid linker helix is shown as a red box. Normalised fluorescence spectra of untreated (blue) and activated (orange) AMPfret are shown. (**C**) Normalised FRET ratio calculated from the curves in panel B, using the same colour code. The AMPfret encoding multigene expression plasmid was transfected into HEK293T (**D**) and 3T3-L1 (**E**) cells and the FRET signal measured over time upon addition of AICAR (1 mM) or 2- deoxy glucose (2-DG, 20 mM). Micrographs of cells imaged in the CFP and YFP channels are shown (scale bars: 50 μm). Adapted from (52).